Observation of Collective Coupling between an Engineered Ensemble of Macroscopic Artificial Atoms and a Superconducting Resonator

Kosuke Kakuyanagi,[1,*] Yuichiro Matsuzaki,[1] Corentin Déprez,[1] Hiraku Toida,[1] Kouichi Semba,[2] Hiroshi Yamaguchi,[1] William J. Munro,[1] and Shiro Saito[1]

[1]*NTT Basic Research Laboratories, NTT Corporation, 3-1 Morinosato-Wakamiya, Atsugi, Kanagawa 243-0198, Japan*

[2]*National Institute of Information and Communications Technology, 4-2-1, Nukuikitamachi, Koganei, Tokyo 184-8795, Japan*

(Received 23 June 2016; published 16 November 2016)

The hybridization of distinct quantum systems is now seen as an effective way to engineer the properties of an entire system leading to applications in quantum metamaterials, quantum simulation, and quantum metrology. Recent improvements in both fabrication techniques and qubit design have allowed the community to consider coupling large ensembles of artificial atoms, such as superconducting qubits, to a resonator. Here, we demonstrate the coherent coupling between a microwave resonator and a macroscopic ensemble composed of several thousand superconducting flux qubits, where we observe a large dispersive frequency shift in the spectrum of 250 MHz. We achieve the large dispersive shift with a collective enhancement of the coupling strength between the resonator and qubits. These results represent the largest number of coupled superconducting qubits realized so far.

DOI: 10.1103/PhysRevLett.117.210503

Quantum science has reached a very interesting stage in its development where we are now beginning to engineer the properties that we require of our quantum systems [1,2]. Hybridization is a core technique in achieving this, as an additional system can be used to greatly change not only the properties of the overall system, but also its environment [3–7]. Specifically, a hybrid system composed of many qubits and a common field such as a cavity mode [8,9] may provide an excellent way of realizing such quantum engineering, leading to quantum applications including the development of quantum simulations [10,11], spin squeezing [12–14], and quantum metamaterials [15–21]. The common field can modify the environment for the qubits [22], which lets us observe interesting many-body phenomena such as quantum phase transitions [23–28], superradiance [29,30], and superabsorption [31,32]. Cavities coupled with atoms, trapped ions, and semiconductor devices are attractive candidates for realizing a hybrid device [33–35]. Although superconducting circuits are a relatively new technology, compared with other devices, they can be easily coupled with heterogenous quantum systems [36–41]. In particular, a number of superconducting resonators have been coupled to electron spin ensembles [42–48]. If we are to investigate quantum many-body phenomena, we will need full control over the ensemble. In most typical superconducting circuit-ensemble hybrid experiments, the ensemble has been formed from a collection of either atoms or molecules (with examples including nitrogen vacancy centers [37,38,45,46], ferromagnetic magnons [47], and bismuth donor spins in silicon [48]). In these cases, the characteristics of the ensemble are set as the ensemble is formed, and are difficult to change. However, we use configurable artificial atoms of superconducting qubits as our ensemble due to their *in situ* tunability.

Superconducting qubits are macroscopic two-level systems with significant design freedoms [49,50]. Josephson junctions provide the superconducting circuit with nonlinearity, and we can tailor the qubit properties by changing the design of the circuit. Frequency tunability [51,52], coherence time control [53], tunable coupling strength [54], engineering selection rules of qubit transitions [55], and control of the level structure of the qubit [56] have been demonstrated with the superconducting qubits. So, compared with natural atoms that are the size of an angstrom, an ensemble of the superconducting qubits has the remarkable potential that control lines can be, in principle, routed to each qubit to tune their individual properties such as a frequency and coupling strength.

Besides the tunability, another key issue in terms of observing interesting quantum phenomena is how to scale the number of the qubits. A microwave cavity has been coupled with multiple superconducting qubits (four transmons [57–59] or eight flux qubits [60]). However, the number of coherently coupled superconducting qubits in the previously reported demonstration may not be large enough for interesting applications. For a smaller number of the qubits, it is possible to simulate the system by a classical computer, while we need a quantum device containing many qubits to explore quantum many-body phenomena such as quantum phase transitions [23–30]. Also, when we use entanglement for a sensitive detection, the difference between the performance of a quantum device and classical one becomes larger as the number of the qubits is increased [12–14,31,32]. So we need to enlarge our system to many more qubits. Here, we

demonstrate the coherent coupling between a microwave resonator and a macroscopic ensemble composed of several thousand superconducting flux qubits, where we observe a large dispersive frequency shift in the spectrum of 250 MHz.

We model our hybrid resonator-qubit ensemble system with the Tavis-Cummings Hamiltonian which can be written in the rotating frame of the microwave driving frequency [61] as

$$H = H_S + H_D + H_I, \tag{1}$$

$$H_S = \hbar(\omega_r - \omega)\hat{a}^\dagger\hat{a} + \frac{\hbar}{2}\sum_{j=1}^{N}(\omega_j - \omega)\hat{\sigma}_{z,j}, \tag{2}$$

$$H_D = \hbar\Omega(\hat{a}^\dagger + \hat{a}), \tag{3}$$

$$H_I = \hbar\sum_{j=1}^{N} g_j(\hat{\sigma}_j^+\hat{a} + \hat{\sigma}_j^-\hat{a}^\dagger), \tag{4}$$

where H_S, H_D, and H_I denote the system Hamiltonian, driving Hamiltonian, and interaction Hamiltonian, respectively. Here, $\hat{a}$ ($\hat{a}^\dagger$) represents the annihilation (creation) operator of the microwave resonator, $\hbar\omega_r$ denotes the energy of the resonator, $\hbar\omega_j = \sqrt{\Delta_j^2 + \epsilon_j^2}$ denotes the energy of the jth flux qubit where Δ_j is the tunneling energy of the jth qubit, $\epsilon_j = 2I_j(\Phi_{\rm ex}^{(j)} - \frac{1}{2}\Phi_0)$ is the energy bias, and N denotes the number of flux qubits. Here, I_j denotes the persistent current of the jth flux qubit, Φ_0 denotes the flux quantum, $\Phi_{\rm ex}^{(j)}$ denotes the applied magnetic flux. Next, Ω denotes a microwave driving field amplitude with a frequency of $\hbar\omega$, $g_j = (\Delta_j/\sqrt{\Delta_j^2 + \epsilon_j^2})g_j'$ represents the effective coupling strength where g_j' represents the bare inductive coupling strength calculated from the persistent currents and inductance of the devices. We rewrite the energy bias as $\epsilon_j = 2I_j(\Phi_{\rm ex} + \delta\Phi_{\rm ex}^{(j)} - \frac{1}{2}\Phi_0) = 2I_j(\Phi_{\rm ex} - \frac{1}{2}\Phi_0) + \epsilon_{0j}$ where $\Phi_{\rm ex}$ denotes the average applied magnetic field and $\epsilon_{0j} = 2I_j\delta\Phi_{\rm ex}^{(j)}$ denotes the energy bias variation caused by the inhomogeneous magnetic flux $\delta\Phi_{\rm ex}^{(j)}$. The operating point of the flux qubits can be tuned by applying the magnetic flux, which results in the change in ϵ and g.

Now, we can calculate the transmitted photon intensity of the microwave resonator as follows. By solving the Heisenberg equations in the steady state limit with a weak coupling regime [62–64], we obtain the transmitted photon intensity $T(\omega)$ (see Supplemental Material [65])

$$|T(\omega)|^2 \simeq \frac{|\Omega|^2}{[\omega - (\omega_r + \delta\omega_r)]^2 + (\gamma_r + \delta\gamma_r)^2}, \tag{5}$$

$$\delta\omega_r = -\sum_{j=1}^{N}\frac{g_j^2(\omega_j - \omega_r)\tanh(\frac{\hbar\omega_j}{2k_BT_E})}{(\omega_j - \omega_r)^2 + \gamma_j^2}, \tag{6}$$

$$\delta\gamma_r = \sum_{j=1}^{N}\frac{g_j^2\gamma_j}{(\omega_j - \omega_r)^2 + \gamma_j^2}, \tag{7}$$

$$\gamma_j = [1 + (e^{(\hbar\omega_j/k_BT_E)} - 1)^{-1}]\gamma_{\rm qubit}, \tag{8}$$

where $\delta\omega_r$ denotes a resonator frequency shift, $\delta\gamma_r$ describes the change in the resonator decay rate, γ_r represents the bare decay rate of the resonator, $\gamma_{\rm qubit}$ (γ_j) describes the relaxation rate of the qubit at zero (finite) temperature, and T_E denotes the environmental temperature. Importantly, $\delta\gamma_r$ tends to increase as the inhomogeneous width of the qubits becomes larger [64].

The ensemble of flux qubits is effected by inhomogeneous broadening, as it is difficult to make homogeneous junctions [67]. The flux qubit has three Josephson junctions, and the area of each junction has a statistical distribution with mean values of $\overline{\beta}_k$ and a standard deviation of σ_k ($k = 1, 2, 3$) for the three junctions. In our modeling, we assume a Gaussian distribution for these. The broadening results in variations in the persistent current and the tunneling energy of the flux qubit. The applied magnetic field is also inhomogeneous, which induces the fluctuation distribution in ϵ_0. It is worth mentioning that g_j' and ϵ_{0j} values are proportional to the I_j value, and so, we can rewrite these as $g_j' = \overline{g}I_j/\overline{I}$ and $\epsilon_{0j} = \epsilon_{0j}'I_j/\overline{I}$ where $\overline{I}$ and $\overline{g}$ denote the average value of the persistent current and coupling strength, respectively. Further, we assume a Gaussian distribution for the value of ϵ_{0j}' with a mean value of zero and a standard deviation of $\delta\epsilon_0'$ (see Supplemental Material [65]).

Now, let us explain our experiment where thousands of superconducting flux qubits are coupled with a superconducting resonator. Since the resonant frequency of the superconducting flux qubits is sensitive to small changes in the fabrication conditions [67], the superconducting flux qubits suffer from inhomogeneous broadening of a few GHz. In principle, we could tune the frequency of individual qubits with control lines routed to them [51,52]. However, even in the current technology, the collective coupling of superconducting flux qubits with a common resonator can overcome this inhomogeneity. The coupling strength $g(\simeq 14.3$ MHz) between the resonator and each qubit is enhanced by $\sqrt{N}$ times where N is the number of flux qubits [68,69], letting us obtain $\sqrt{N}g$ as a collective coupling strength. This results in N times enhancement for the dispersive frequency shift of the resonator, allowing us to observe the signal of the coupling even under the effect of the inhomogeneous broadening.

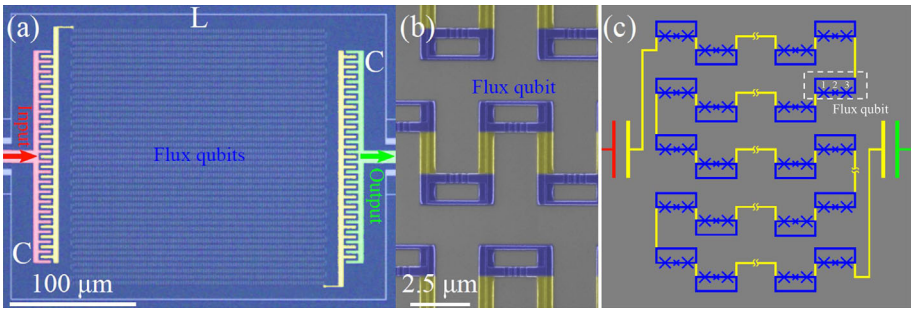

FIG. 1. Our hybrid device is composed of 4300 superconducting flux qubits embedded in an LC resonator. These flux qubits are coupled with the resonator via mutual inductance. We show in (a) an optical microscope image, (b) a scanning electron micrograph (in false colors), and (c) a schematic view of our device where a flux qubit has three junctions with one of them being smaller than the other. Spectroscopy is performed on this device by measuring the photons transmitted from the resonator.

We fabricated two samples of a microwave resonator coupled with 4300 flux qubits on a Si wafer where each sample has a different alpha value [67]. The flux qubits share an edge with the inductor line of the resonator. The flux qubit consists of a loop interrupted by three Al-Al_2O_3-Al Josephson junctions. We designed the area of one junction to be α times smaller than those of the other two junctions. The value of E_J/E_c is 75 where E_J (E_c) denotes a Josephson (charge) energy. Our experimental setup is shown in Fig. 1. We measure the microwave transmission properties of the resonator system by a network analyzer. The sample was placed in a dilution refrigerator operating at 20 mK. We can apply magnetic fields perpendicular to the flux qubits, and this can change the operating point of the flux qubit. Further, we can change the temperature from below 10 mK (base temperature) to 230 mK by a heater (see Supplemental Material [65] for details).

Spectroscopy was performed on the resonator coupled with thousands of flux qubits for the two separate devices (samples A and B) with different designed α values. The frequency of maximum transmission indicates the resonance of our device composed of superconducting flux qubits and a microwave resonator where we vary the driving microwave frequency. In our experiment, we observed a resonator frequency shift due to coupling with the flux qubits. One of the sample shows a negative frequency shift of the resonator [Fig. 2(a)]. This suggests

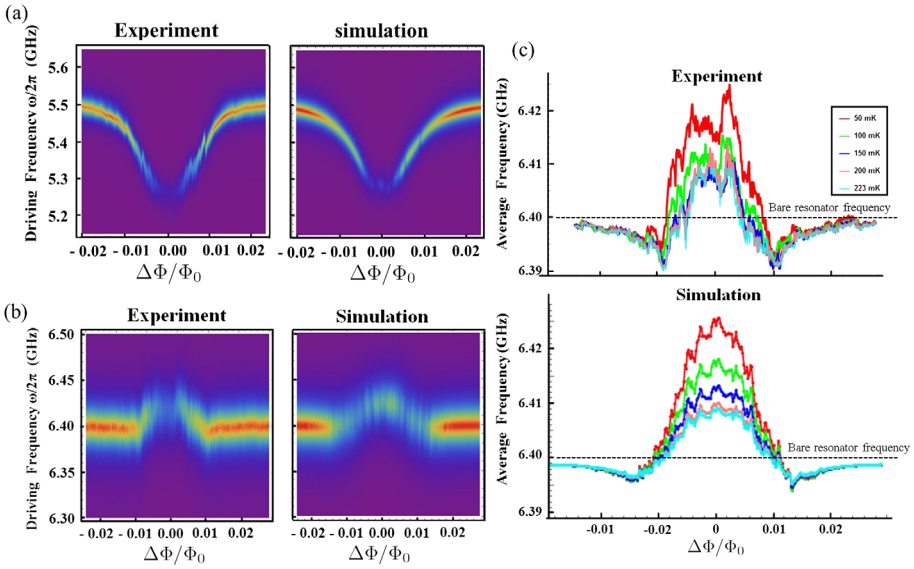

FIG. 2. Experimental results and numerical simulations of the energy spectrum of a microwave resonator coupled to an ensemble of flux qubits. For sample A, we used the parameters $N = 4300$, $\bar{\beta}_2/\bar{\beta}_1 = 0.6285$, $\bar{\beta}_1 = \bar{\beta}_3 = 1$, $\sigma_1/\bar{\beta}_1 = \sigma_2/\bar{\beta}_2 = \sigma_3/\bar{\beta}_3 = 0.025$, $\omega_{\rm res}/2\pi = 5.5$ GHz, $\bar{g}'/2\pi = 14.3$ MHz, $\delta\epsilon_0'/2\pi = 2.8$ GHz, $\gamma_{\rm qubit}/2\pi = 50$ MHz, and $\gamma_r/2\pi = 13.3$ MHz. For sample B, we used the parameters $N = 4300$, $\bar{\beta}_2/\bar{\beta}_1 = 0.7815$, $\bar{\beta}_1 = \bar{\beta}_3$, $\sigma_1/\bar{\beta}_2 = \sigma_2/\bar{\beta}_2 = \sigma_3/\bar{\beta}_3 = 0.055$, $\omega_{\rm res}/2\pi = 6.4$ GHz, $\bar{g}'/2\pi = 9.2$ MHz, $\delta\epsilon_0'/2\pi = 2.6$ GHz, $\gamma_{\rm qubit}/2\pi = 50$ MHz, and $\gamma_r/2\pi = 12.2$ MHz. (c) Temperature dependence of the energy spectrum of a microwave resonator coupled to thousands of flux qubits. We use the same parameters as those in Fig. 2. From the top, we plot the results with $T_E = 50$ mK (red), $T_E = 100$ mK (green), $T_E = 150$ mK (blue), $T_E = 200$ mK (pink), $T_E = 223$ mK (cyan).

that the tunneling energy of the flux qubits is larger than the resonator frequency. The other sample shows both positive and negative frequency shifts in the spectrum [Fig. 2(b)]. This can occur when the tunneling energy of the flux qubits is smaller than the resonator frequency. In such a case, the flux-qubit energy can cross the resonator frequency by applying a magnetic field. Although we cannot observe the vacuum Rabi splitting of the qubit-resonator anticrossing due to our large inhomogeneous broadening of a few GHz, the frequency shift indicates the collective coupling between them. We also measured the temperature dependence of the resonator frequency where we plot the frequency of the resonator in the spectroscopic measurements [Fig. 2(c)]. This shows that an increase in the temperature tends to suppress the frequency shift of the resonator. This demonstrates that we can control the strength of the collective coupling.

For sample A, we have observed a large negative resonator-frequency shift of $\delta\omega_r/2\pi \simeq 250$ MHz, and we reproduce this with our model [Fig. 2(a)]. From our modeling, the mean value (standard deviation) of the tunneling energy of the flux qubits is estimated as $\overline{\Delta}/2\pi = 9.74$ GHz ($\sigma_\Delta/2\pi = 1.7$ GHz). The negative resonator-frequency shift of $\delta\omega_{\rm res}/2\pi \simeq 250$ MHz can be understood as the dispersive energy shift [8,70]. Since this experiment is implemented in a dilution refrigerator with a temperature of 50 mK, the flux qubit is prepared in the ground state as long as the qubit energy is much larger than the thermal energy of $k_B T/2\pi\hbar \simeq 1$ GHz. When most of the flux qubit energy is well above the resonator frequency, each qubit induces a negative resonator frequency shift of $-|g_j|^2/(\omega_j - \omega_r)$. Because of a collective effect that occurs as an enhancement of a coupling strength when qubits are coupled with a common mode [68,69], we can achieve a large dispersive shift of $\delta\omega_{\rm res}/2\pi \simeq 250$ MHz for sample A. Although the individual coupling $\overline{g}'/2\pi (= 14.3$ MHz) is small, the collective effect enhances the coupling strength $\sqrt{N}$ times [68,69]. Because of the inhomogeneously broadened ensemble of the qubit, the width of the hybrid device's resonance feature becomes larger as the energy bias of the flux qubits approach zero as shown in Fig. 2(a). This can be understood as follows. As the operating point of the flux qubits approaches the optimal one, the detuning between the flux qubit and the resonator becomes smaller, while the coupling between them becomes larger, and this induces additional decay in the resonator due to the inhomogeneous broadening of the flux qubits.

Importantly, these experimental results provide an order estimation of the number of flux qubits coupled with the resonator. The bare coupling strength between a single flux qubit and the resonator is described as $g_j' = M_{qr} I_j \sqrt{\omega_r/2\hbar L}$ where L denotes the inductance of the resonator and M_{qr} denotes a mutual inductance between the flux qubit and the resonator. We can estimate these values as $M \simeq 10$ pH and $L \simeq 100$ nH from numerical simulations, and so we obtain $g_j'/2\pi \simeq 16$ MHz for $\omega_r/2\pi = 5.5$ GHz and $I_j = 250$ nA. On the other hand, by reproducing the spectroscopic measurements in Fig. 2, we estimate the average bare coupling strength as $\overline{g}'/2\pi \simeq 14.3$ MHz where we assume $N = 4300$. This small discrepancy in the estimated coupling strength of g_j' might indicate that, although we intended to fabricate 4300 flux qubits, some of them would not work as qubits because of imperfect fabrication. This could mean that the actual number of flux qubits contributing to the collective enhancement might be smaller than 4300. However, from these estimations, we can at least conclude that thousands of flux qubits should be involved in the collective coupling with the resonator, because otherwise, experimental results such as the large dispersive shift of $\delta\omega_{\rm res}/2\pi \simeq 250$ MHz cannot be explained by the parameters $N < 1000$ and $g_j'/2\pi \simeq 16$ MHz.

For sample B, we observed both a negative and a positive frequency shift of tens of MHz, and we can reproduce the experimental spectroscopic results with our theoretical model [Fig. 2(b)]. From these theoretical calculations, the mean value (standard deviation) of the tunneling energy of the flux qubits is estimated to be $\overline{\Delta}/2\pi = 1.17$ GHz ($\sigma_\Delta/2\pi = 1.1$ GHz). Since this is smaller than $\omega_{\rm res}$, the average frequency of the flux qubits can match the resonator frequency when an appropriate amount of the magnetic flux is applied on the flux qubits. It is worth mentioning that, as the operating point approaches the optimal one, the coupling strength becomes stronger in our model. This results in both a larger frequency shift and an additional broadening effect on the resonator spectrum. The latter can be explained by a stronger coupling with the noisy qubit ensemble that suffers from inhomogeneous broadening. The dispersive frequency shift of the resonator around the optimal point for sample B is $\delta\omega_{\rm res}/2\pi \simeq 16$ MHz, which is much smaller than the shift observed in sample A. This is due to the small tunneling energy ($\overline{\Delta}/2\pi \sim 1$ GHz) of the flux qubit where the thermal energy depolarizes the flux qubit, which weakens the dispersive shift.

We can reproduce the temperature dependence of the spectroscopic measurements with our model as shown in Fig. 2(c). The temperature dependence becomes clearer as the flux qubit approaches the optimal point where the energy of the flux qubit reaches its minimum. This can be understood as follows. When the thermal energy is much larger than the flux qubit energy, the state of the flux qubits becomes an almost completely mixed state, and half of the flux qubits induce a positive dispersive shift, while the other flux qubits induce a negative dispersive shift, which cancels out the collective enhancement of the coupling strength. So our experiment demonstrates a control of the strength of the collective coupling by changing the temperature. On the other hand, when the energy bias of the flux qubit becomes large, the resonator frequency shift becomes almost independent of the temperature because the flux qubit is not significantly effected by the thermal effect.

Interestingly, on top of the dispersive shift, we observe numerous small energy shifts in the spectroscopy in the experiments and simulations [see Fig. 2(c)]. These peaks are reproducible over multiple experiments, and so, they do not correspond to noise. In the limit of a large number of qubits coupled with the resonator, we should observe the dispersive frequency shift and/or vacuum Rabi splitting in the spectroscopy, because we can consider the qubit ensemble to be a single harmonic oscillator by the continuum limit [64]. On the other hand, when the resonator is coupled with the large but finite number of the flux qubits in our experiment, the discrete nature of each flux qubit induces such numerous additional peaks.

In conclusion, we have reported experiments to show collective coupling between a superconducting resonator and an ensemble of superconducting flux qubits. We have observed the large dispersive frequency shift of the resonator, and this demonstrates a collective behavior of the superconducting qubits. Our analysis indicates that thousands of superconducting qubits contribute to the coupling. These results represent the largest number of coupled superconducting qubits realized so far. Our system has a number of potential applications. Such applications include quantum field sensing, where the flux qubit ensemble can be squeezed via the interaction with the resonator [12–14]. Superradiance [30] and superabsorption [31,32] is another, where entanglement between the flux qubits plays an essential role to emit or absorb resonator photons in a collective way. Demonstration of these phenomena would require only global control and could realistically be implemented in our device.

We thank S. Endo, I. Natsuko, and N. Lambert for their useful comments. This work was supported by JSPS KAKENHI Grants No. 15K17732 and No. 25220601. This work was also partly supported by MEXT KAKENHI Grants No. 15H05869 and No. 15H05870.

*kakuyanagi.kosuke@lab.ntt.co.jp

[1] J. P. Dowling and G. J. Milburn, Phil. Trans. R. Soc. A **361**, 1655 (2003).
[2] T. D. Ladd, F. Jelezko, R. Laflamme, Y. Nakamura, C. Monroe, and J. L. OBrien, Nature (London) **464**, 45 (2010).
[3] Z.-L. Xiang, S. Ashhab, J. You, and F. Nori, Rev. Mod. Phys. **85**, 623 (2013).
[4] S. C. Benjamin, B. W. Lovett, and J. M. Smith, Laser Photonics Rev. **3**, 556 (2009).
[5] J. P. Paz, Nature (London) **412**, 869 (2001).
[6] Y. Matsuzaki, X. Zhu, K. Kakuyanagi, H. Toida, T. Shimo-Oka, N. Mizuochi, K. Nemoto, K. Semba, W. J. Munro, H. Yamaguchi, and S. Saito, Phys. Rev. Lett. **114**, 120501 (2015).
[7] S. Putz, A. Angerer, D. O. Krimer, R. Glattauer, W. J. Munro, S. Rotter, J. Schmiedmayer, and J. Majer, arXiv: 1512.00248.
[8] A. Blais, J. Gambetta, A. Wallraff, D. I. Schuster, S. M. Girvin, M. H. Devoret, and R. J. Schoelkopf, Phys. Rev. A **75**, 032329 (2007).
[9] D. I. Tsomokos, S. Ashhab, and F. Nori, New J. Phys. **10**, 113020 (2008).
[10] S. Schmidt and J. Koch, Ann. Phys. (Berlin) **525**, 395 (2013).
[11] I. Georgescu, S. Ashhab, and F. Nori, Rev. Mod. Phys. **86**, 153 (2014).
[12] M. Kitagawa and M. Ueda, Phys. Rev. A **47**, 5138 (1993).
[13] S. D. Bennett, N. Y. Yao, J. Otterbach, P. Zoller, P. Rabl, and M. D. Lukin, Phys. Rev. Lett. **110**, 156402 (2013).
[14] T. Tanaka, P. Knott, Y. Matsuzaki, S. Dooley, H. Yamaguchi, W. J. Munro, and S. Saito, Phys. Rev. Lett. **115**, 170801 (2015).
[15] N. I. Zheludev, Science **328**, 582 (2010).
[16] C. M. Soukoulis and M. Wegener, Nat. Photonics **5**, 523 (2011).
[17] N. I. Zheludev and Y. S. Kivshar, Nat. Mater. **11**, 917 (2012).
[18] M. Ricci, N. Orloff, and S. M. Anlagea, Appl. Phys. Lett. **87**, 034102 (2005).
[19] N. Lazarides and G. Tsironis, Appl. Phys. Lett. **90**, 163501 (2007).
[20] S. M. Anlage, J. Opt. **13**, 024001 (2011).
[21] P. Jung, S. Butz, S. V. Shitov, and A. V. Ustinov, Appl. Phys. Lett. **102**, 062601 (2013).
[22] E. M. Purcell, Phys. Rev. **69**, 681 (1946).
[23] K. Hepp and E. H. Lieb, Ann. Phys. (N.Y.) **76**, 360 (1973).
[24] Y. K. Wang and F. Hioe, Phys. Rev. A **7**, 831 (1973).
[25] C. Emary and T. Brandes, Phys. Rev. E **67**, 066203 (2003).
[26] N. Lambert, Y. N. Chen, R. Johansson, and F. Nori, Phys. Rev. B **80**, 165308 (2009).
[27] N. Lambert, C. Emary, and T. Brandes, Phys. Rev. Lett. **92**, 073602 (2004).
[28] L. J. Zou, D. Marcos, S. Diehl, S. Putz, J. Schmiedmayer, J. Majer, and P. Rabl, Phys. Rev. Lett. **113**, 023603 (2014).
[29] R. H. Dicke, Phys. Rev. **93**, 99 (1954).
[30] V. V. Temnov and U. Woggon, Phys. Rev. Lett. **95**, 243602 (2005).
[31] K. Higgins, S. Benjamin, T. Stace, G. Milburn, B. W. Lovett, and E. Gauger, Nat. Commun. **5**, 4705 (2014).
[32] M. Maragkou, Nat. Photonics **8**, 813 (2014).
[33] J.-M. Raimond, M. Brune, and S. Haroche, Rev. Mod. Phys. **73**, 565 (2001).
[34] D. Wineland, C. Monroe, W. Itano, D. Leibfried, B. King, and D. Meekhof, J. Res. Natl. Inst. Stand. Technol. **103**, 259 (1998).
[35] T. Yoshie, A. Scherer, J. Hendrickson, G. Khitrova, H. Gibbs, G. Rupper, C. Ell, O. Shchekin, and D. Deppe, Nature (London) **432**, 200 (2004).
[36] D. Marcos, M. Wubs, J. M. Taylor, R. Aguado, M. D. Lukin, and A. S. Sørensen, Phys. Rev. Lett. **105**, 210501 (2010).
[37] X. Zhu, S. Saito, A. Kemp, K. Kakuyanagi, S. Karimoto, H. Nakano, W. Munro, Y. Tokura, M. Everitt, K. Nemoto, M. Kasu, N. Mizuochi, and K. Semba, Nature (London) **478**, 221 (2011).
[38] S. Saito, X. Zhu, R. Amsüss, Y. Matsuzaki, K. Kakuyanagi, T. Shimo-Oka, N. Mizuochi, K. Nemoto, W. J. Munro, and K. Semba, Phys. Rev. Lett. **111**, 107008 (2013).

[39] X. Zhu, Y. Matsuzaki, R. Amsuss, K. Kakuyanagi, T. Shimo-Oka, N. Mizuochi, K. Nemoto, W. J. Munro, K. Semba, and S. Saito, Nat. Commun. **5**, 3424 (2014).
[40] A. D. OConnell, M. Hofheinz, M. Ansmann, R. C. Bialczak, M. Lenander, E. Lucero, M. Neeley, D. Sank, H. Wang, M. Weides, J. Wenner, J. M. Martinis, and A. N. Cleland, Nature (London) **464**, 697 (2010).
[41] P.-B. Li, Z.-L. Xiang, P. Rabl, and F. Nori, Phys. Rev. Lett. **117**, 015502 (2016).
[42] Y. Kubo, F. R. Ong, P. Bertet, D. Vion, V. Jacques, D. Zheng, A. Dréau, J. F. Roch, A. Auffeves, F. Jelezko, J. Wrachtrup, M. F. Barthe, P. Bergonzo, and D. Esteve, Phys. Rev. Lett. **105**, 140502 (2010).
[43] R. Amsüss, C. Koller, T. Nöbauer, S. Putz, S. Rotter, K. Sandner, S. Schneider, M. Schramböck, G. Steinhauser, H. Ritsch, J. Schmiedmayer, and J. Majer, Phys. Rev. Lett. **107**, 060502 (2011).
[44] D. Schuster, A. Sears, E. Ginossar, L. DiCarlo, L. Frunzio, J. Morton, H. Wu, G. Briggs, B. Buckley, D. Awschalom *et al.*, Phys. Rev. Lett. **105**, 140501 (2010).
[45] Y. Kubo, C. Grezes, A. Dewes, T. Umeda, J. Isoya, H. Sumiya, N. Morishita, H. Abe, S. Onoda, T. Ohshima, V. Jacques, A. Dreau, J. F. Roch, I. Diniz, A. Auffeves, D. Vion, D. Esteve, and P. Bertet, Phys. Rev. Lett. **107**, 220501 (2011).
[46] S. Putz, D. O. Krimer, R. Amsüss, A. Valookaran, T. Nöbauer, J. Schmiedmayer, S. Rotter, and J. Majer, Nat. Phys. **10**, 720 (2014).
[47] Y. Tabuchi, S. Ishino, A. Noguchi, T. Ishikawa, R. Yamazaki, K. Usami, and Y. Nakamura, Science **349**, 405 (2015).
[48] A. Bienfait, J. J. Pla, Y. Kubo, M. Stern, X. Zhou, C. C. Lo, C. D. Weis, T. Schenkel, M. L. W. Thewalt, D. Vion, D. Esteve, B. Julsgaard, K. Molmer, J. J. L. Morton, and P. Bertet, Nat. Nanotechnol. **11**, 253 (2016).
[49] J. Clarke and F. Wilhelm, Nature (London) **453**, 1031 (2008).
[50] Y. Makhlin, G. Schön, and A. Shnirman, Rev. Mod. Phys. **73**, 357 (2001).
[51] F. G. Paauw, A. Fedorov, C. J. P. M. Harmans, and J. E. Mooij, Phys. Rev. Lett. **102**, 090501 (2009).
[52] X. Zhu, A. Kemp, S. Saito, and K. Semba, Appl. Phys. Lett. **97**, 102503 (2010).
[53] M. Reed, B. Johnson, A. Houck, L. DiCarlo, J. Chow, D. Schuster, L. Frunzio, and R. Schoelkopf, Appl. Phys. Lett. **96**, 203110 (2010).
[54] A. Niskanen, K. Harrabi, F. Yoshihara, Y. Nakamura, S. Lloyd, and J. Tsai, Science **316**, 723 (2007).
[55] K. Harrabi, F. Yoshihara, A. O. Niskanen, Y. Nakamura, and J. S. Tsai, Phys. Rev. B **79**, 020507 (2009).
[56] K. Inomata, K. Koshino, Z. R. Lin, W. D. Oliver, J. S. Tsai, Y. Nakamura, and T. Yamamoto, Phys. Rev. Lett. **113**, 063604 (2014).
[57] J. M. Fink, R. Bianchetti, M. Baur, M. Göppl, L. Steffen, S. Filipp, P. J. Leek, A. Blais, and A. Wallraff, Phys. Rev. Lett. **103**, 083601 (2009).
[58] J. A. Mlynek, A. A. Abdumalikov, Jr, J. M. Fink, L. Steffen, M. Baur, C. Lang, A. F. van Loo, and A. Wallraff, Phys. Rev. A **86**, 053838 (2012).
[59] M. Feng, Y. Zhong, T. Liu, L. Yan, W. Yang, J. Twamley, and H. Wang, Nat. Commun. **6**, 7111 (2015).
[60] P. Macha, G. Oelsner, J.-M. Reiner, M. Marthaler, S. André, G. Schön, U. Hübner, H.-G. Meyer, E. Ilichev, and A. V. Ustinov, Nat. Commun. **5**, 5146 (2014).
[61] M. Tavis and F. W. Cummings, Phys. Rev. **170**, 379 (1968).
[62] C. W. Gardiner and P. Zoller, *Quantum Noise* (Springer, Berlin, 2004).
[63] M. J. Collett and C. W. Gardiner, Phys. Rev. A **30**, 1386 (1984).
[64] I. Diniz, S. Portolan, R. Ferreira, J. M. Gérard, P. Bertet, and A. Auffeves, Phys. Rev. A **84**, 063810 (2011).
[65] See Supplemental Material at http://link.aps.org/supplemental/10.1103/PhysRevLett.117.210503 for the approximation that we use in our calculation, which includes Ref. [66].
[66] R. Houdré, R. P. Stanley, and M. Ilegems, Phys. Rev. A **53**, 2711 (1996).
[67] T. P. Orlando, J. E. Mooij, L. Tian, C. H. van der Wal, L. Levitov, S. Lloyd, and J. J. Mazo, Phys. Rev. B **60**, 15398 (1999).
[68] A. Imamoğlu, Phys. Rev. Lett. **102**, 083602 (2009).
[69] J. H. Wesenberg, A. Ardavan, G. A. D. Briggs, J. J. L. Morton, R. J. Schoelkopf, D. I. Schuster, and K. Mølmer, Phys. Rev. Lett. **103**, 070502 (2009).
[70] A. Wallraff, D. Schuster, A. Blais, L. Frunzio, R. Huang, J. Majer, S. Kumar, S. Girvin, and R. Schoelkopf, Nature (London) **431**, 162 (2004).